Supporting Information

Lamellar Flower-Like Porous MoS_2 as an Efficient Cocatalyst to Boost Photocatalytic Hydrogen Evolution of CdS

Lei Su, Lulu Luo, Junwen Wang, Tao Song, Weixia Tu*, and Zhou-jun Wang*

State Key Laboratory of Organic-Inorganic Composites, Beijing University of Chemical Technology, Beijing 100029, China

* Corresponding authors. E-mail: tuwx@mail.buct.edu.cn; wangzj@mail.buct.edu.cn.

Table of Contents

Characterization

The crystal structure was obtained by X-ray diffraction (XRD) using a Bruker D8 Advance diffractometer (Bruker AXS Ltd.) with Cu-Kα radiation. Nitrogen (N_2) adsorption-desorption isotherms were taken on a Quantachrome Autosorb iQ surface area analyzer at -196 °C. Scanning electron microscope (SEM) pictures were obtained from a S-4700F facility (JEOL Ltd.). Transmission electron microscope (TEM) photos were taken from a J-3010 instrument (JEOL Ltd.). A spectrophotometer (Tu-1901 Beijing General Instrument Co., Ltd.) was utilized to obtain the Ultraviolet-visible (UV-vis) diffuse reflectance spectra (DRS) using $BaSO_4$ as the reflectance background. X-ray photoelectron spectroscopy (XPS) spectra were obtained on a VG ESCALAB 250 spectrometer (Thermo Fisher Ltd.). The charging effect of powder samples in XPS was calibrated by C 1s (284.8 eV) of the adventitious carbon contamination. The element analysis was characterized on an inductively coupled plasma spectrometry-atomic emission spectrometer (ICP-AES, ULTIMA, JY Inc.). Photoluminescence spectra (PL) profiles were obtained on a F-7000 spectrophotometer (Hitachi Co., Ltd.). Photo-electrochemical characterizations were carried out using a CHI760E instrument in a standard three-electrode system. The counter electrode was Pt slice and the reference electrode was $Hg/HgCl_2$. The electrolyte was Na_2SO_4 aqueous solution (0.5 M). 2 mg sample was added into a mixture of Nafion (50 μl) and ethanol (1 ml). The obtained solution was then sonicated for 30 min. After that, fluorine-doped tin oxide (FTO) glass (1.5 × 1.5 cm^2) was covered with the above solution (40 μl) as the working electrodes. A 300 W Xe lamp was used as the light source ($\lambda \geq 420$ nm).

Table S1. Comparison of photocatalytic activities for H_2 evolution on various MoS_2/CdS composites.

Photocatalyst	Catalyst amount (mg)	Scavenger	Light source	Amount of H_2 evolution (mmol h^{-1} g^{-1})	Ref.
MoS_2/CdS	3	Lactic Acid	300 W Xe lamp ($\lambda \geq 420$ nm)	54.1	This work
MoS_2/CdS	20	Lactic Acid	300 W Xe lamp ($\lambda \geq 420$ nm)	39.7	S1
MoS_2/CdS	20	Lactic Acid	300 W Xe lamp ($\lambda \geq 420$ nm)	38.75	S2
MoS_2/CdS	20	Lactic Acid	300 W Xe lamp ($\lambda \geq 400$ nm)	26.65	S3
MoS_2/CdS	20	Lactic Acid	300 W Xe lamp ($\lambda \geq 350$ nm)	26.14	S4
MoS_2/CdS	50	Na_2S-Na_2SO_3	300 W Xe lamp ($\lambda \geq 420$ nm)	17.2	S5
MoS_2/CdS	100	Lactic Acid	300 W Xe lamp ($\lambda \geq 420$ nm)	13.15	S6
MoS_2/CdS	50	Lactic Acid	300 W Xe lamp ($\lambda \geq 420$ nm)	12.38	S7
MoS_2/CdS	10	Lactic Acid	300 W Xe lamp ($\lambda \geq 420$ nm)	11.85	S8
MoS_2/CdS	100	Lactic Acid	300 W Xe lamp ($\lambda \geq 420$ nm)	10.85	S9
MoS_2/CdS	50	Lactic Acid	300 W Xe lamp ($\lambda \geq 420$ nm)	6.1	S10

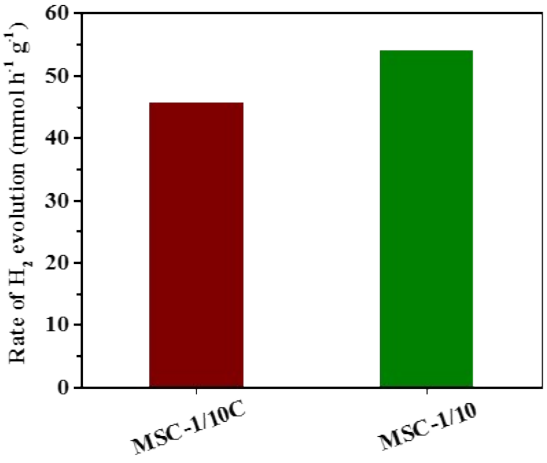

Fig. S1 H_2 evolution rates of the MSC-1/10C and MSC-1/10 photocatalysts.

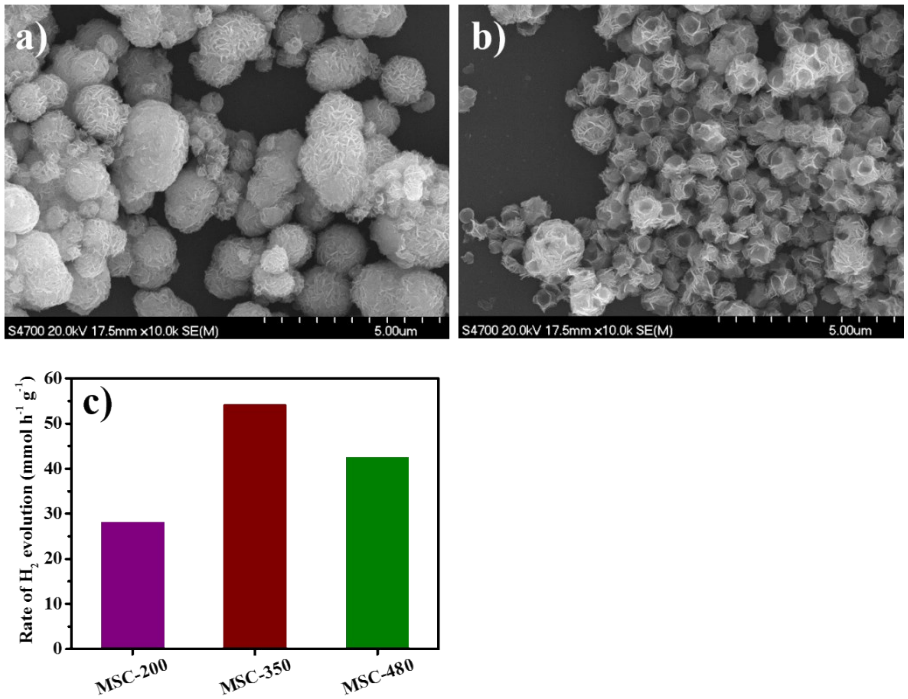

Fig. S2 SEM images of porous MoS_2-200 (a) and porous MoS_2-480 (b) as well as photocatalytic H_2 evolution activities of various porous MoS_2/CdS composites (c).

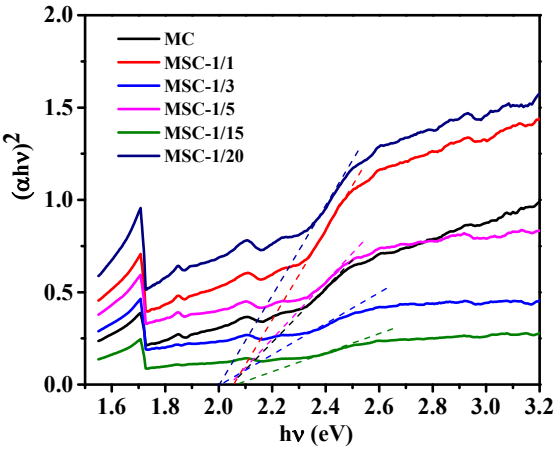

Fig. S3 The Tauc plots to determine band gaps of various porous MoS_2/CdS composites.

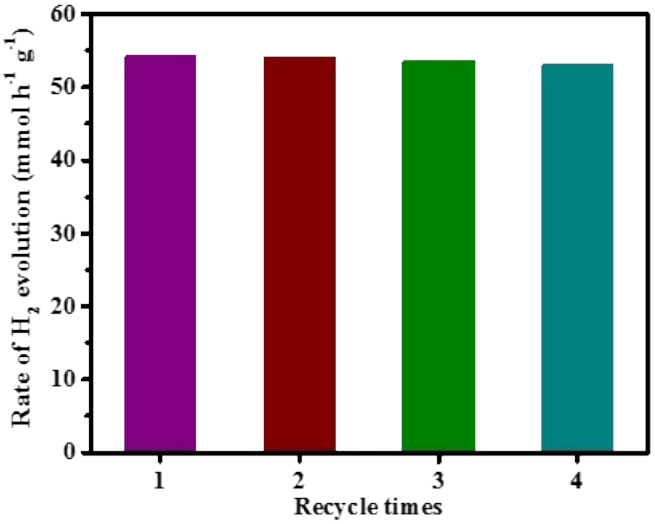

Fig. S4 Recycling runs of the porous MoS_2/CdS composite (30% MSC) for H_2 evolution.

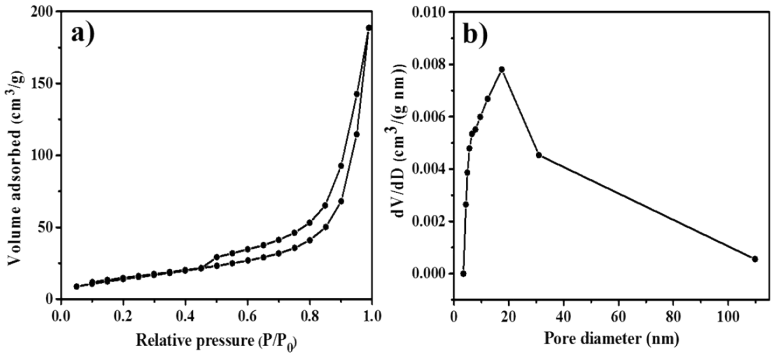

Fig. S5 N_2 adsorption-desorption isotherms and pore diameter distribution curves of the porous MoS_2/CdS composite.

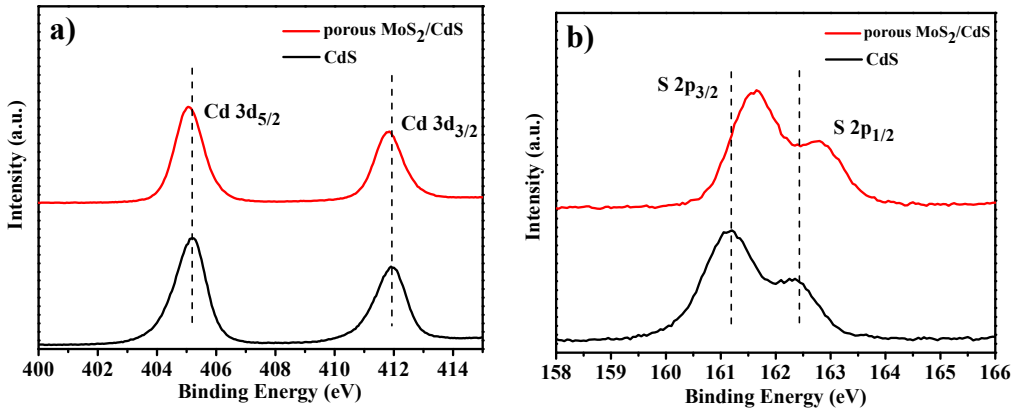

Fig. S6 Cd 3d (a) and S 2p XPS spectra of the porous MoS_2/CdS composite in comparison with CdS.

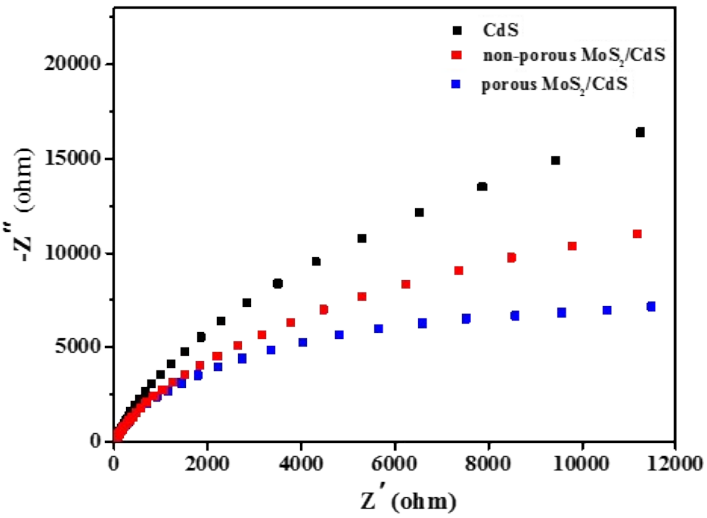

Fig. S7 Electrochemical impedance spectra of the sample electrodes containing CdS, non-porous MoS_2/CdS and porous MoS_2/CdS.

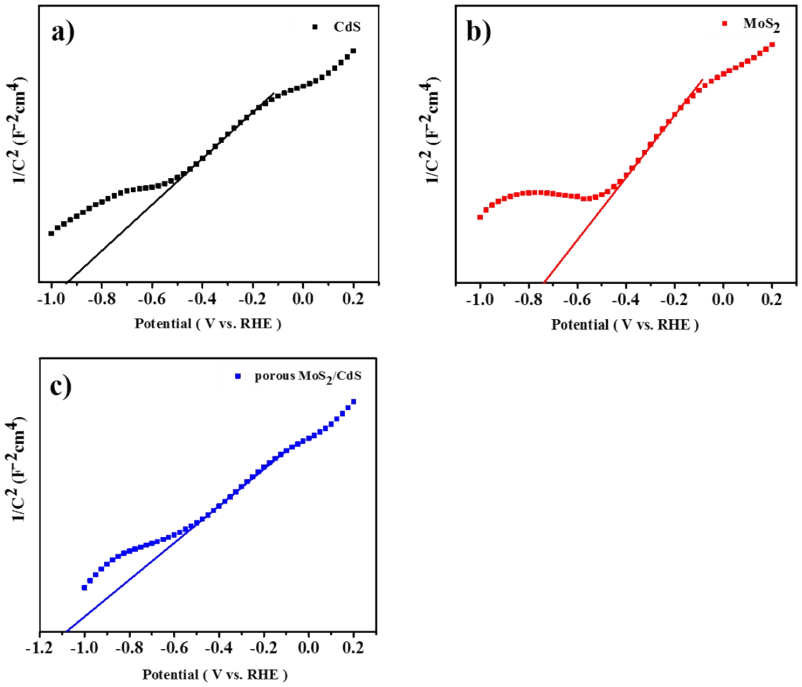

Fig. S8 Mott-Schottky results of CdS (a), MoS_2 (b) and porous MoS_2/CdS composite (c).

References

(S1) P. Du, Y. Zhu, J. Zhang, D. Xu, W. Peng, G. Zhang, F. Zhang and X. Fan, *RSC Adv.,* 2016**, 6**, 74394-74399.

(S2) A. Wu, C. Tian, Y. Jiao, Q. Yan, G. Yang and H. Fu, *Appl. Catal. B*, 2017, **203**, 955-963.

(S3) B. Han, S. Liu, N. Zhang, Y.-J. Xu and Z.-R. Tang, *Appl. Catal. B*, 2017, **202***,* 298-304.

(S4) Y. Yang, Y. Zhang, Z. Fang, L. Zhang, Z. Zheng, Z. Wang, W. Feng, S. Weng, S. Zhang and P. Liu, *ACS Appl. Mater. Inter.*, 2017, **9**, 6950-6958.

(S5) S. Zhang, H. Yang, H. Gao, R. Cao, J. Huang and X. Xu, *ACS Appl. Mater. Inter.*, 2017, **9**, 23635-23646.

(S6) G. Chen, D. Li, F. Li, Y. Fan, H. Zhao, Y. Luo, R. Yu and Q. Meng, *Appl. Catal. A,* 2012**, 443-444**, 138-144.

(S7) C. Feng, Z. Chen, J. Hou, J. Li, X. Li, L. Xu, M. Sun and R. Zeng, *Chem. Eng. J.*, 2018, **345**, 404-413.

(S8) R. K. Chava, J. Y. Do and M. Kang, *Appl. Surf. Sci.,* 2018, **433**, 240-248.

(S9) H. Lin, Y. Li, H. Li and X. Wang, *Nano Res.*, 2017, **10**, 1377-1392.

(S10) Y. Peng, J. Li, X. Qian, J. Zhang and J. Lin, *J. Nanopart. Res.,* 2018**, 20**, 104.